THE JOURNAL OF BIOLOGICAL CHEMISTRY VOL. 280, NO. 43, pp. 35836–35842, October 28, 2005

A Picrotoxin-specific Conformational Change in the Glycine Receptor M2–M3 Loop*

Received for publication, June 20, 2005, and in revised form, August 16, 2005 Published, JBC Papers in Press, August 18, 2005, DOI 10.1074/jbc.M506645200

Rebecca Hawthorne and Joseph W. Lynch[1]

From the School of Biomedical Sciences, University of Queensland, Brisbane, Queensland 4072, Australia

The external loop linking the M2 and M3 transmembrane domains is crucial for coupling agonist binding to channel gating in the glycine receptor chloride channel (GlyR). A substituted cysteine accessibility scan previously showed that glycine activation increased the surface accessibility of 6 contiguous residues (Arg^{271}–Lys^{276}) toward the N-terminal end of the homomeric α1 GlyR M2–M3 loop. In the present study we used a similar approach to determine whether the allosteric antagonist, picrotoxin, could impose conformational changes to this domain that cannot be induced by varying agonist concentrations alone. Picrotoxin slowed the reaction rate of a sulfhydryl-containing compound (MTSET) with A272C, S273C, and L274C. Before interpreting this as a picrotoxin-specific conformational change, it was necessary to eliminate the possibility of steric competition between picrotoxin and MTSET. Accordingly, we showed that picrotoxin and the structurally unrelated blocker, bilobalide, were both trapped in the R271C GlyR in the closed state and that a point mutation to the pore-lining $Thr^{6'}$ residue abolished inhibition by both compounds. We also demonstrated that the picrotoxin dissociation rate was linearly related to the channel open probability. These observations constitute a strong case for picrotoxin binding in the pore. We thus conclude that the picrotoxin-specific effects on the M2–M3 loop are mediated allosterically. This suggests that the M2–M3 loop responds differently to the occupation of different binding sites.

The glycine receptor chloride channel (GlyR)[2] mediates inhibitory neurotransmission in the central nervous system (1, 2). Like other members of the cysteine-loop ligand-gated ion channel (LGIC) family, functional GlyRs comprise 5 subunits arranged symmetrically around a central ion-conducting pore. Each subunit consists of a large extracellular ligand-binding domain followed by 4 α-helical transmembrane domains, termed M1–M4 (3, 4).

It is now well established that the extramembranous loop joining M2 and M3 is crucial for transmitting the agonist-induced conformational change to the M2 domain activation gate (5–8). Consistent with this role, a substituted cystine accessibility study on the α1 GlyR showed that the surface accessibility of 6 contiguous cysteine-substituted residues in this loop (Arg^{271} to Lys^{276}) was increased in the open state (9). Thus, the conformational status of the M2–M3 loop depends on the degree to which the receptor is activated by agonist. However, it is not known whether allosteric modulators could impose conformational changes to this loop that cannot be induced by simply varying the agonist concentration alone. This is an important question as it could reveal a hitherto unexpected complexity in the role of this important domain. In particular, it would address the hypothesis that the M2–M3 loop conformation can be modified in different ways by different ligands.

In this study we address this question by determining whether the closure of the channels by the allosteric inhibitor, picrotoxin (PTX), preserves the relationship between domain conformation and fractional peak current magnitude that is seen in its absence. If this relationship is not preserved, we would conclude that the PTX-induced closed state is conformationally different from the unliganded closed state.

PTX inhibits most anionic LGICs including the recombinant α homomeric GlyR, the GABA type-A receptor ($GABA_AR$), and the invertebrate glutamate receptor Cl^- channel (GluClR). PTX is a use-dependent inhibitor of $GABA_AR$ (10) and GluClR (11), but displays no use dependence at the α homomeric GlyR (12). PTX inhibition is extremely sensitive to mutations to residues at the 2′ and 6′ pore-lining positions (11, 13–18). Although this implies that PTX binds in the pore, it is unlikely that picrotoxin inhibition is because of classic pore block. Data obtained using a variety of techniques including single channel kinetic and conductance analysis (10, 19), macroscopic current kinetic analysis (20), interactions between picrotoxin analogs (21), site-directed mutagenesis (12, 22), and combined fluorescence labeling and electrophysiology (23) together form a strong case that PTX allosterically inhibits anionic LGICs. PTX may be a useful modulator for the present investigation as mutations in the M2–M3 loop have profound effects on its mode of action (12).

MATERIALS AND METHODS

Mutagenesis and Expression of Human GlyR α1 Subunit cDNAs—Site-directed mutations were incorporated as previously described (9). The WT and mutant GlyRs investigated in this study incorporated the functionally silent C41A mutation (9). Plasmid constructs were transiently transfected into HEK293 cells via the calcium phosphate precipitation method. Cells were washed 24 h later, and currents were recorded over the next 72 h.

Patch Clamp Electrophysiology—Currents were measured using whole cell recording at a holding potential of −40 mV using an Axopatch 1D amplifier (Axon Instruments, Foster City, CA), and data were directly recorded to disk using pCLAMP 6 or 9 software (Axon Instruments). Cells were perfused with the standard bathing solution containing (in mM): 140 NaCl, 5 KCl, 2 $CaCl_2$, 1 $MgCl_2$, 10 HEPES, 10 glucose, pH 7.4. Patch pipettes had tip resistances of ~1.5 MΩ when filled with the standard intracellular solution containing (in mM): 145 CsCl, 2 $CaCl_2$, 2 $MgCl_2$, 10 HEPES, 10 EGTA, pH 7.4. PTX and bilobalide (BB) (both from Sigma) were stored as 10–100 mM stock solutions in Me_2SO for up to 3 months and dissolved into the bath solution on the day of the experiment. Methanethiosulfonate ethyltrimethylammonium (MTSET), from Toronto Research Chemicals (Toronto, Canada), was prepared as

* This work was supported by the Australian Research Council. The costs of publication of this article were defrayed in part by the payment of page charges. This article must therefore be hereby marked "*advertisement*" in accordance with 18 U.S.C. Section 1734 solely to indicate this fact.

[1] To whom correspondence should be addressed. Tel.: 617-3365-3157; Fax: 617-3365-1766; E-mail: j.lynch@uq.edu.au.

[2] The abbreviations used are: GlyR, glycine receptor chloride channel; BB, bilobalide; DTT, dithiothreitol; EC, equivalent concentration; $GABA_AR$, γ aminobutyric acid type A receptor chloride channel; GluClR, glutamate receptor chloride channel; LGIC, ligand-gated ion channel; MTSET, methanethiosulfonate ethyltrimethylammonium; PTX, picrotoxin; WT, wild type.

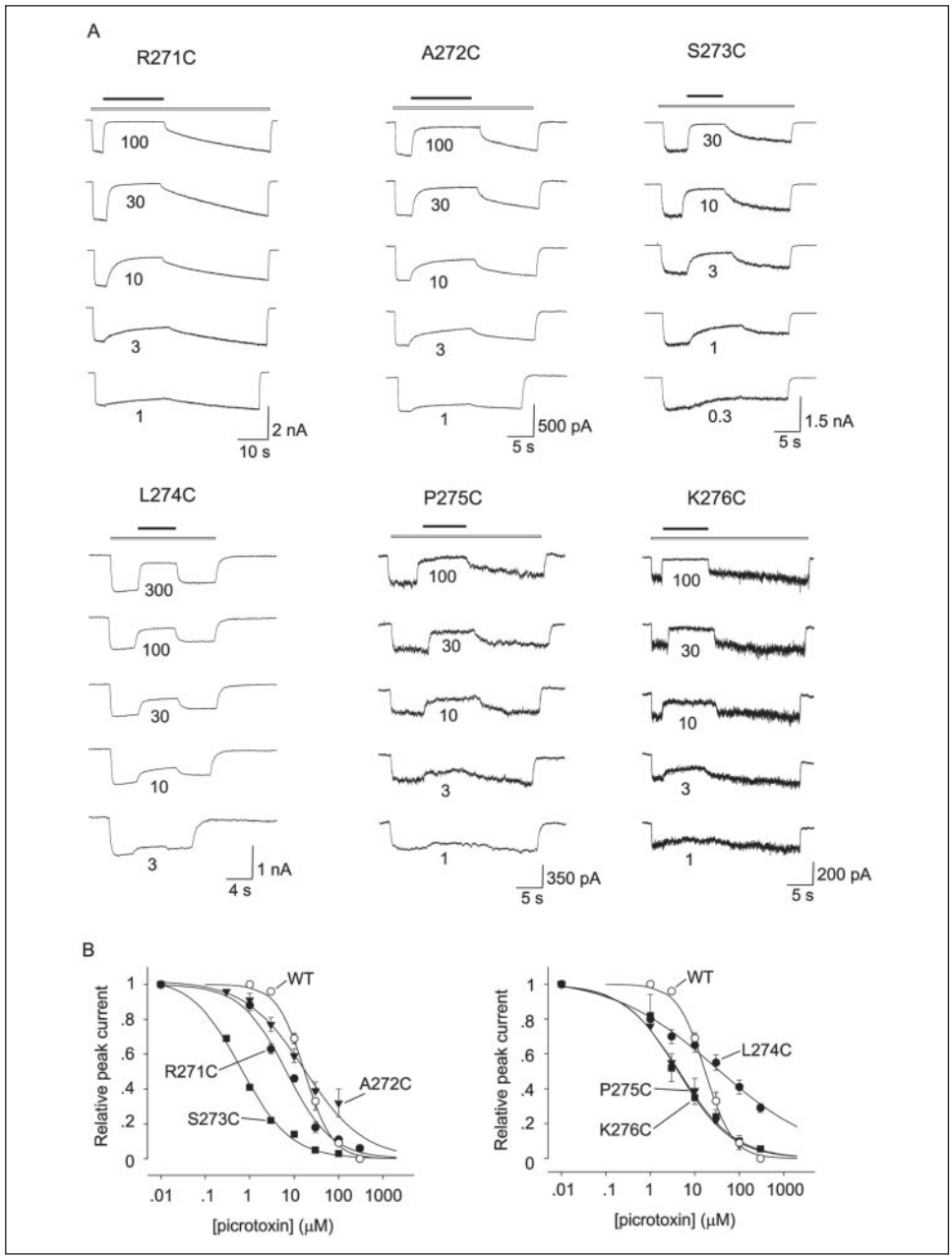

FIGURE 1. **PTX dose-response curves.** *A*, examples of the effects of various PTX concentrations on glycine currents recorded from cells expressing the indicated mutant GlyR. The glycine concentration used to activate each receptor is shown in TABLE ONE. *B*, averaged PTX dose-response curves from the WT GlyR, plus the R271C, A272C, and S273C GlyRs (*left panel*), and the L274C, P275C, and K276C GlyRs (*right panel*). The parameters of best fit averaged from individual dose-response curves are summarized in TABLE ONE.

a stock solution of 10 mM in distilled water and maintained on ice for up to 3 h until used. It was applied to cells within 30 s of being dissolved into room temperature bathing solution. The disulfide reducing agent, dithiothreitol (DTT) was prepared daily as a 1 mM solution in the standard bathing solution. Solutions were applied to cells via a parallel system of gravity-fed tubes, and solution exchange was effected with a time constant of about 100 ms. Experiments were performed at room temperature (19–22 °C).

The effects of MTSET on glycine-gated currents were tested as follows. Prior to MTSET application, cells were bathed in 1 mM DTT for 1 min to ensure that exposed sulfhydryl groups were fully reduced. Then the glycine dose response was measured at least 3 times over a period of ~10 min to ensure that EC_{10} and EC_{30} glycine concentrations could reliably be chosen and that the current magnitude was invariant (±5%) prior to the application of MTSET. Following application of the MTSET-containing solution, cells were washed in control solution for at least 2 min before the current magnitudes were measured again. This was done to ensure that cysteine modification had taken place. Currents were then reduced to their original control levels by a 1-min exposure to 1–2 mM DTT.

Data Analysis—Results are expressed as mean ± S.E. of three or more independent experiments. The empirical Hill equation, fitted by a non-linear least squares algorithm (Sigmaplot 9.0, Systat Software Inc, Richmond, CA), was used to calculate the 50% effective concentrations for PTX inhibition (IC_{50}) and the Hill coefficient (n_H) values. Exponential fits were performed using the same non-linear least squares algorithm. Statistical significance was determined by Student's paired or unpaired *t* test (as indicated) with $p < 0.05$ representing significance.

RESULTS

PTX Interactions with the M2–M3 Loop—The peak current magnitudes and glycine EC_{50} values for all mutant GlyRs examined in this study have previously been published (9). Because the present study concerns the effects of PTX on M2–M3 loop conformation, it was first

TABLE ONE

PTX sensitivity of WT and mutant GlyRs

GlyR	[Glycine][a]	PTX		
		IC_{50}	n_H	n
	mM	μM		
WT	0.03	18 ± 1	1.5 ± 0.1	5
R271C	3	7.1 ± 0.9[b]	0.77 ± 0.07[b]	8
A272C	3	17 ± 6	0.58 ± 0.09[b]	4
S273C	0.04	0.68 ± 0.04[b]	0.78 ± 0.05[b]	3
L274C	0.25	103 ± 26[b]	0.52 ± 0.07[b]	4
P275C	2	5.0 ± 1.4[b]	0.78 ± 0.09[b]	4
K276C	3	4.9 ± 1.6[b]	0.60 ± 0.06[b]	4

[a] This shows the glycine concentration used to measure PTX dose responses.
[b] Significantly different from WT value using an unpaired *t* test ($p < 0.05$).

necessary to measure the mean PTX IC_{50} and n_H values for the WT and all cysteine-substituted GlyRs. Sample recordings from cells expressing each mutant GlyR examined in this study are shown in Fig. 1*A*. These show the effects on increasing concentrations of PTX on currents activated by EC_{30}-EC_{50} glycine concentrations. Averaged PTX dose responses are displayed in Fig. 1*B* (separated into two panels for clarity) and the mean IC_{50} and n_H values are summarized in TABLE ONE, together with the glycine concentration at which each was measured. These results reveal two general features. First, as shown in TABLE ONE, the n_H values for all cysteine mutants were <1, which is significantly less than the n_H value for the WT GlyR of around 1.5. These results imply that PTX inhibits the WT GlyR in a cooperative manner, but that this cooperativity is lost when mutations are incorporated into the N-terminal half of the M2–M3 loop. Mutagenesis also significantly increased the PTX sensitivity of most mutants, except for A272C where there was no significant difference, and L274C where there was an ~5-fold reduction in PTX sensitivity. In agreement with a previous report (12), these results indicate that loop mutations affect the allosteric actions of PTX, but they provide no evidence for the direct disruption of a PTX binding site.

Our original aim was to determine the effect of PTX on the MTSET reactivity of cysteines introduced individually to positions 271–276 in the α1 GlyR. We previously demonstrated that the MTSET reaction rates for all cysteine-substituted mutants are increased in the channel open state (9). To assess the effect of PTX on cystine accessibility, we first measured the MTSET reaction rates of all mutants at the EC_{10} and EC_{30} glycine concentrations. (As MTSET reaction rate is proportional to the degree of receptor activation, we expect this to increase with increasing glycine concentration.) We then added a sufficient concentration of PTX to the EC_{30} glycine concentration to inhibit the current to the EC_{10} current magnitude. If the MTSET reaction rate depends only on the channel open probability, then the reaction rates in the presence of PTX + EC_{30} glycine should be identical to its reaction rate in the presence of EC_{10} glycine. However, if the respective reaction rates are different, it may be possible to conclude that PTX promotes a conformational state that cannot be attained by glycine.

An example of such an experiment performed on the S273C mutant GlyR is shown in Fig. 2*A*. All traces in this figure are from the same cell. The *upper left panel* shows the effect of 100 μM MTSET applied in the presence of an EC_{10} (in this case 30 μM) concentration of glycine. A 2-min wash in control solution had no effect, although the MTSET-induced current increase was completely reversed by a 1-min exposure to 1 mM of the reducing agent, DTT (Fig. 2*A*). These observations confirm that MTSET acted via a covalent modification of S273C. The time course of the MTSET-induced current change was adequately fitted by

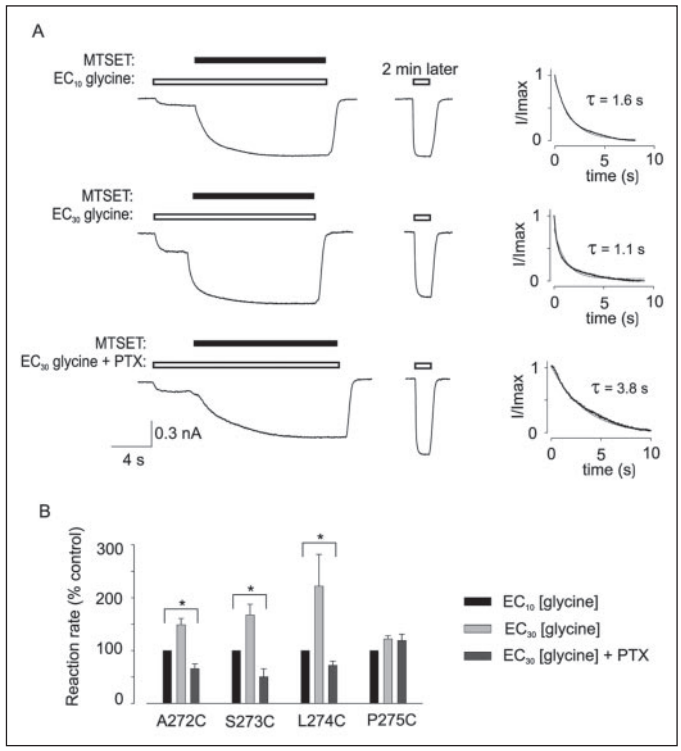

FIGURE 2. **Effect of PTX on the MTSET reactivity of mutant GlyRs.** *A*, all data in this panel were recorded from the same cell expressing the S273C GlyR. In this and all subsequent figures, the time course of glycine and MTSET application are shown by the *unfilled* and *filled bars*, respectively. MTSET was applied at a concentration of 100 μM in all experiments unless otherwise stated. In this cell, the glycine EC_{10} and EC_{30} concentrations were 50 and 70 μM, respectively. The *upper* and *middle traces* show current responses to MTSET at EC_{10} and EC_{30} glycine concentrations, respectively, and the *bottom trace* shows the effect of simultaneous application of MTSET, EC_{30} glycine, and 5 μM PTX. Single exponential fits to the MTSET-induced current change are displayed in the *right panel*. A control glycine application 2 min after MTSET reaction indicates the effect is irreversible. Traces in the *upper*, *middle*, and *lower panels* are separated by 1-min applications of 1 mM DTT. *B*, summary of changes in MTSET reaction rate associated with the three experimental conditions as depicted in *A*. All reaction rates are normalized to the value recorded in the presence of EC_{10} glycine. Data for S273C were averaged from 3 cells, and a Student's paired *t* test reveals a significant difference between the EC_{10} glycine reaction rate and the EC_{30} glycine + 5 mM PTX reaction rate ($p < 0.05$). Statistical significance is denoted by the *asterisk*. A similar analysis was performed on all other mutants and the mean results are displayed for A272C ($n = 4$ cells), L274C ($n = 4$ cells), and P275C ($n = 5$ cells).

a single exponential with a time constant of 1.6 s (*upper right panel*). The corresponding current changes in the presence of EC_{30} glycine alone or EC_{30} glycine + 10 μM PTX were fitted by time constants of 1.1 and 3.8 s, respectively (Fig. 2*A*, *middle* and *lower panels*). The same experimental protocol was applied to 2 other cells expressing the S273C mutant GlyR and the averaged results are summarized in Fig. 2*B*. These results are normalized to the MTSET reaction rate measured in the presence of EC_{10} glycine. A paired *t* test ($p < 0.05$) indicates that 10 μM PTX + EC_{30} glycine caused a significant reduction in the MTSET reaction rate with S273C relative to that caused by EC_{10} glycine (Fig. 2*B*).

We used a similar protocol to examine the effect of PTX on MTSET reaction rates with the R271C, A272C, L274C, P275C, and K276C mutant GlyRs. In the A272C and L274C mutant GlyRs, PTX + EC_{30} glycine also caused a significant reduction in the reaction rate relative to that seen in the presence of EC_{10} glycine alone (Fig. 2*B*). However, in the P275C GlyR, the reaction rate in PTX + EC_{30} glycine was not significantly different to that obtained with EC_{10} glycine (Figs. 2*B* and 3*A*). This negative result was confirmed in each of 5 cells, and the averaged results are shown in Fig. 2*B*. This result is not surprising as the reaction rate differential between the closed state and EC_{30} glycine-activated

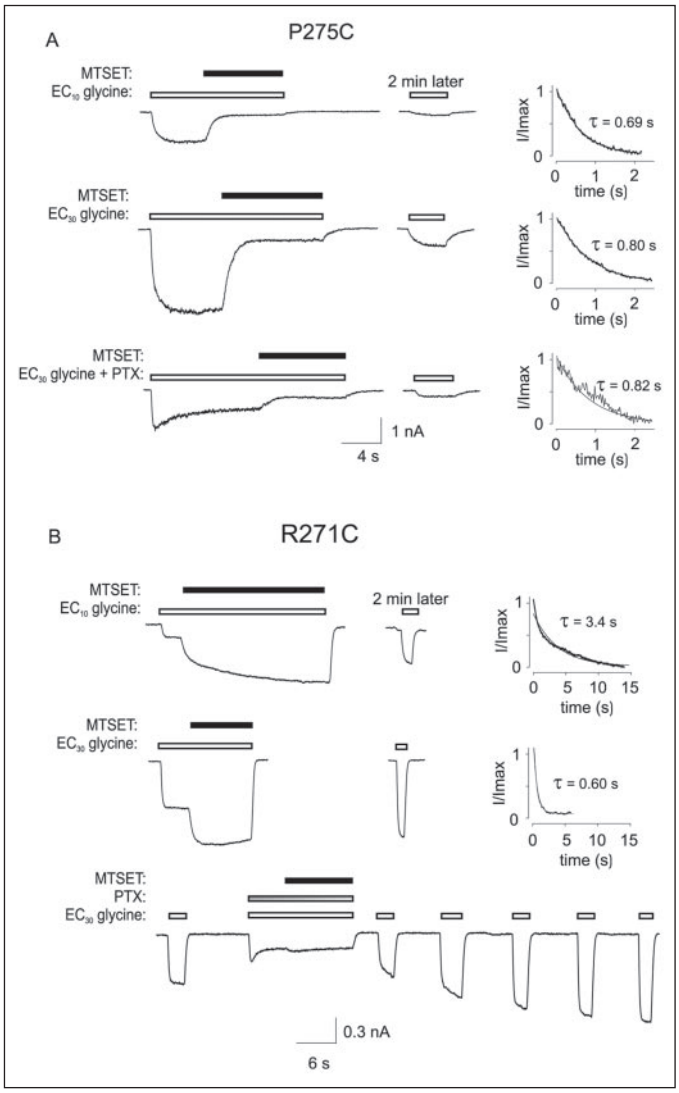

FIGURE 3. **Sample results for P275C and R271C using the protocol as described in the legend to Fig. 2A.** *A*, all data in this panel were recorded from a cell expressing the P275C GlyR. In this cell, glycine was applied at 1 and 3 mM (corresponding to EC_{10} and EC_{30}), and PTX was applied at 10 μM. Note the apparent lack of effect of glycine concentration and PTX on MTSET reaction rates. Data averaged from 5 cells confirms this (Fig. 2*B*). *B*, all data in this panel were recorded from a cell expressing the R271C GlyR. The experimental protocol in the *upper 2 panels* was the same as in Fig. 2A. In this cell, glycine was applied at 1 and 3 mM, and PTX was applied at 10 μM. In the *bottom panel*, control glycine applications before and after MTSET reveal that MTSET did induce a current increase that became apparent only after PTX washout.

state in this mutant is less than 3-fold (9), implying that the surface exposure of P275C varies little during gating.

The effects of PTX on MTSET reactivity of R271C and K276C could not be measured. As shown in the example in Fig. 3*B*, an increase in the R271C reaction rate was observed as the glycine concentration was increased from EC_{10} to EC_{30}. Surprisingly, however, PTX abolished the change in current that otherwise occurs upon the addition of MTSET to these mutants (Fig. 3*B*, *bottom trace*). A similar lack of effect was observed in each of 4 cells expressing the R271C GlyR and in 4 cells expressing the K276C GlyR. There are 2 likely explanations for this. One is that MTSET cannot reach its reaction site in the presence of PTX and the other is that MTSET modification caused an increase in PTX sensitivity, so that the enhanced PTX inhibition exactly cancelled out the MTSET-induced current increase. If both MTSET and PTX are removed following simultaneous exposure, the magnitude of the glycine-activated current increases to the same value as seen following exposure to MTSET in the absence of PTX (Fig. 3*B*, compare *center* and *bottom traces*). This indicates that MTSET modification has taken place and that MTSET modification must therefore cause an increased PTX sensitivity in the R271C GlyR. This was tested directly by measuring the degree of inhibition induced by 10 μM PTX on currents activated by 3 mM glycine both before and after MTSET modification. Before MTSET, PTX inhibited currents to 51 $\pm$ 3% of control, but in the same 4 cells after MTSET modification, it inhibited currents to 28 $\pm$ 7% of control. This difference was statistically significant ($p < 0.05$) using a paired t test. A similar experiment performed on the K276C GlyR yielded a similar result. A 10 mM PTX concentration inhibited currents activated by 5 mM glycine to a level of 35 $\pm$ 6% before MTSET modification and to 10 $\pm$ 3% after modification. Again, this difference was statistically significant using a paired t test ($n = 4$ cells, $p < 0.05$). Hence, it is concluded that the lack of current change upon simultaneous application of MTSET + PTX can be attributed to an MTSET-induced increase in PTX sensitivity.

The conclusion thus far is that PTX reduces the reaction rate of MTSET with A272C, S273C, and L274C. There are 3 possible ways by which this could be achieved. The first is that PTX and MTSET may form a complex in free solution. This possibility was eliminated by showing that the PTX IC_{50} for the WT GlyR was not significantly affected by the presence of 1 mM MTSET (not shown). The second possibility is that PTX changes the conformation of this domain via an allosteric action. The third is that PTX binds to either this domain or a nearby domain and sterically interferes with the MTSET reaction. To discriminate between these two possibilities, it is essential to identify the location of the PTX binding site.

PTX Interactions with the Pore—During the course of the above experiments, we noticed that recovery from PTX inhibition required the R271C GlyR to be activated by glycine. This effect is characterized formally in Fig. 4. Fig. 4A shows a control in which 2 applications of an EC_{50} (3 mM) concentration of glycine spaced ~60 s apart are similar in magnitude. Fig. 4*B* shows the slow recovery that follows the complete inhibition of this current by a saturating (300 μM) concentration of PTX. If both glycine and PTX are simultaneously removed when the current is inhibited, it is apparent that recovery from PTX inhibition commences only when glycine is applied 60 s later (Fig. 4*C*). Thus, PTX is "trapped" in the absence of glycine. As shown in the *inset*, overlay of the PTX inhibition recovery phases recorded in Fig. 4, *B* and *C*, reveal identical time courses of recovery. When PTX is applied in the closed state (Fig. 4*D*), a subsequent application of glycine indicates that PTX cannot efficiently access its inhibitory site. Identical experiments to these were performed in each of 5 cells, and the results are summarized in Fig. 4, *E* and *F*. Fig. 4*E* shows the percentage of original current that was observed 65 s after the initial glycine current was terminated for the four experimental conditions depicted in Fig. 4, *A–D*. The 0- and 65-s time points are indicated by the *vertical dashed line*. Fig. 3*E* reveals that the only condition that causes a significant decrease in glycine current at the 65-s time point is when PTX is trapped for 60 s in the closed state. Fig. 3*F* measures the ratio of currents from 5 cells measured at 1-s intervals during the recovery from PTX inhibition following trap relative to the current recorded at the same recovery time point without trap. As there is no substantial deviation from 1 at any point, we conclude that the recovery rate following the 60-s trap is no different from its recovery rate without trap. We also observed PTX trap in the MTSET-modified R271C GlyR and the K276C GlyR ($n = 3$ for each, data not shown), but not in any other mutant GlyR tested in this study.

PTX has long been hypothesized to bind in the GlyR pore (24). However, as discussed below, the evidence supporting this is not overwhelm-

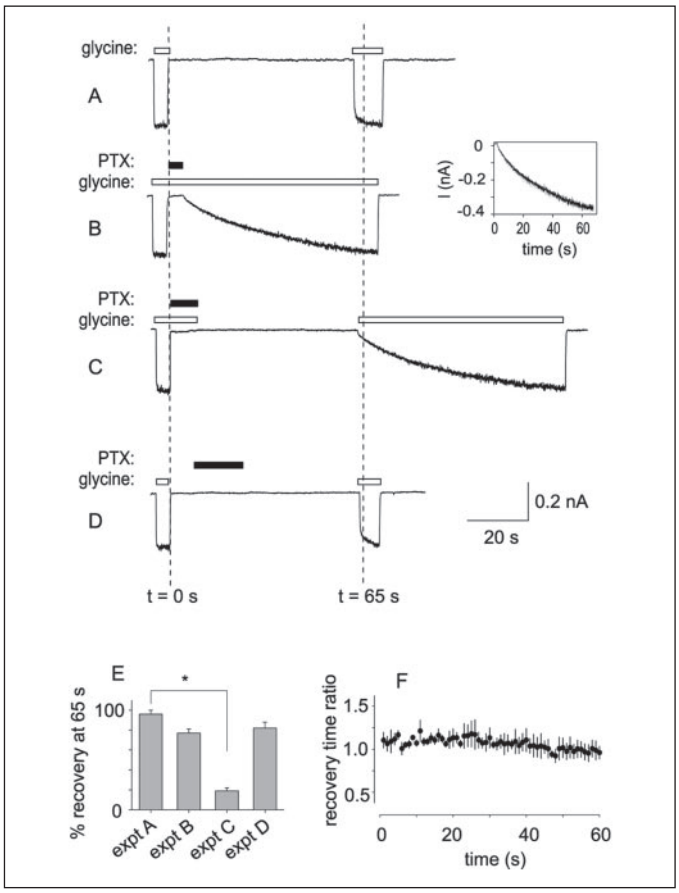

FIGURE 4. **PTX trap in the R271C GlyR.** *A*, all data in *A–D* were from the same cell. Glycine was applied throughout at 3 mM and PTX at 300 μM. *Panel A* shows 2 control glycine applications spaced 60 s apart. *B*, glycine was applied as shown by the *unfilled bar*, and PTX was applied as indicated by the *filled bar*. Note the slow recovery from PTX inhibition. *C*, similar experiment to *B* except that glycine and PTX were simultaneously removed once PTX inhibition reached steady-state. Glycine was reapplied ~60 s later revealing the PTX trap. The *inset* shows the overlaid recovery current time courses from *panels B* and *C*. *D*, PTX applied in the closed state does not cause significant trap. *E*, the mean current amplitude at the 65-s time point is expressed as a percentage of the control current magnitude for the four experimental conditions depicted in *panels A–D*. The 0- and 65-s time points are shown by the *vertical dashed lines*. All experiments were averaged from 5 cells, and only experiment *B* caused a significant ($p < 0.05$) current decrease at 65 s. This measure indicates that the results summarized in *A–D* were typical of those obtained in all cells tested. *F*, the magnitude of the current at 1-s intervals during recovery from trap is expressed as a ratio of the current at the corresponding time point during recovery without trap. All points are averaged from 5 cells. The plot reveals no significant difference in their respective recovery time courses.

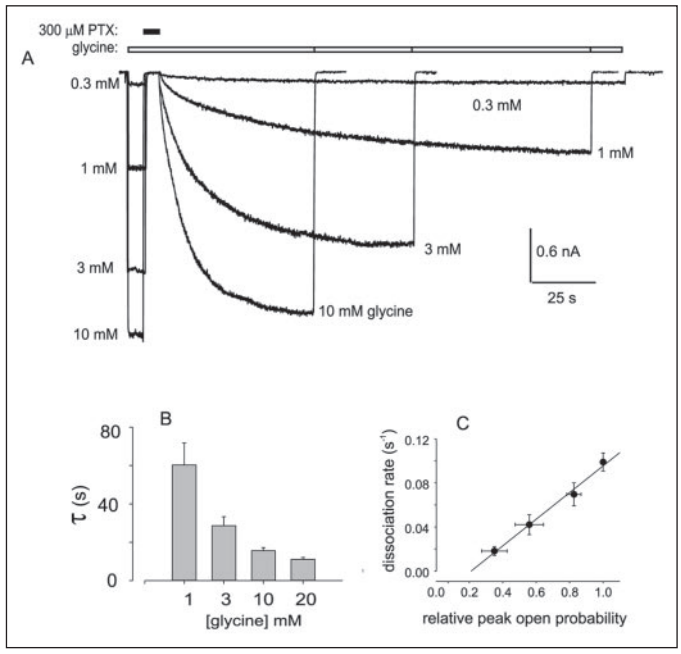

FIGURE 5. **Glycine concentration-dependence of the PTX inhibition recovery rate in the R271C GlyR.** *A*, all data were from the same cell. Currents activated by the indicated glycine concentrations were completely inhibited by 300 μM PTX, and the time course of recovery was compared at the same glycine concentrations. *B*, the current recovery phase was fitted with a single exponential. Results pooled from 4 cells reveal a consistent relationship between recovery time constant (τ) and glycine concentration. *C*, for each recovery curve, the recovery rate ($= 1/\tau$) was plotted against the current at which it was recorded expressed as a fraction of the maximum saturating current. (Saturation occurs at 20 mM glycine in this mutant.) The *points* from *left* to *right* in this plot represent pooled data recorded at 1, 3, 10, and 20 mM glycine, respectively. Linear regression analysis of all individual data points (not of the averaged data as plotted here) reveals a regression coefficient of 0.79.

ing. Nevertheless, on the basis of the PTX trap observation, we retained the hypothesis that PTX binds in the pore, and we designed several experiments to test this.

The first of these is summarized in Fig. 5. We reasoned that if PTX can escape from the R271C GlyR pore in the open state only, then its recovery rate should be proportional to the channel open probability. To test this, currents activated by 0.3, 1, 3, 10, and 20 mM glycine were completely inhibited by 300 μM PTX and the time course of the recovery current was recorded. An example of one such experiment is displayed in Fig. 5*A*. The number of exponential terms needed to adequately fit the recovery phase varied from cell to cell because of the variable presence of a small rapidly recovering current component. As a maximum of around 10% of the current recovers by this fast pathway, it is ignored for the purpose of this analysis and a single exponential curve was fit only to the remaining slow recovery phase. The time constants averaged from 4 cells reveal a consistent relationship between recovery rate and glycine concentration (Fig. 5*B*). The same data are plotted in a different way in Fig. 5*C*. In this analysis, we made use of the fact that 20 mM glycine is saturating at the R271C GlyR (9). We then expressed the current magnitudes activated by 1, 3, and 10 mM as a fraction of the saturating current in each cell and plotted this against the inverse of the dissociation time constant (*i.e.* dissociation rate). The pooled results, displayed in Fig. 5*C*, were well fitted by a linear regression with a regression coefficient of 0.79, implying a linear relation between the PTX unbinding rate and channel open probability. Such a relationship is expected for a molecule than can escape from its site only in the open state. However, this linearity is disrupted at open probabilities less than around 0.2, implying that PTX cannot easily escape during the fast opening events typical of weakly liganded GlyRs (25).

We then reasoned that if PTX is trapped in the pore of the R271C GlyR, then other putative pore-blocking substances with unrelated structures should also be trapped. There are two families of molecules that block GlyRs: cyanotriphenylborate (26) and several structurally related extracts from *Ginkgo biloba* leaves (27, 28). In this study, we used the sesquiterpene trilactone Ginkgo component, BB. Sample responses to increasing concentrations of BB on WT GlyR currents are shown in Fig. 6*A* (*left panel*), and the averaged dose response pooled from 4 cells is shown in Fig. 6*A* (*right panel*). The mean BB IC_{50} was 19.6 ± 1.6 μM and the n_H value was 0.58 ± 0.06 (both $n = 4$). As the *G. biloba* derivatives have only been tested on native GlyRs with unknown subunit compositions, it was first necessary to confirm that BB inhibited the recombinantly expressed GlyR α homomer in a use-dependent manner. This was performed as indicated in Fig. 6*B*. The *upper* and *lower left panels* show the effects of 10 μM BB applied in the *closed* and *open states*, respectively. As seen in the *lower panel*, glycine-induced current activation following BB removal is slow as a result of the slow dissociation of

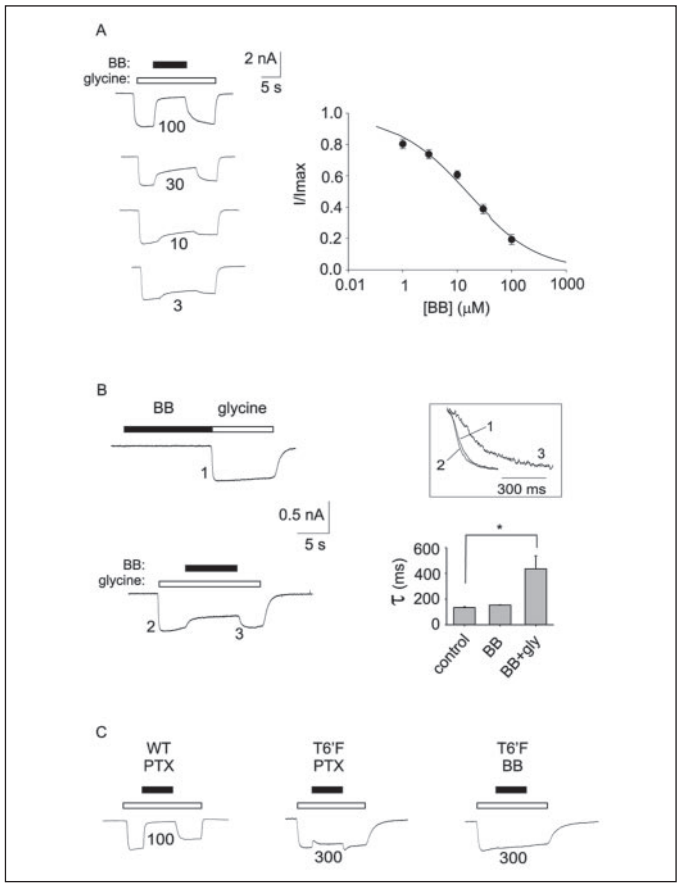

FIGURE 6. **BB effects on the WT and T6′F GlyRs.** *A*, effects of the indicated concentrations of BB on currents activated by 30 μM glycine in cell expressing WT GlyRs. The *right panel* shows the mean BB dose response averaged from 4 cells. The parameters of best fit averaged from individual dose responses are given in the text. *B*, use-dependence of BB inhibition. The *upper left panel* shows a 15-s pre-exposure to 10 μM BB followed immediately by 200 μM application of glycine. The *lower left panel*, from the same cell, shows a control where BB is applied in the open state. The *upper right panel* shows the expanded, normalized glycine-induced activation phases corresponding to points *1*, *2*, and *3* in the *left panel*. *Curve 3* reveals a slower glycine activation rate caused by the slow rate of BB dissociation. Activation time constants averaged from 4 cells are displayed in the *lower right panel*. They show the time constants of glycine-induced activation following cell exposure to control solution (*left column*), BB alone (*center column*), or BB + glycine (*right column*). BB significantly ($p < 0.01$, paired *t* test) inhibited the glycine activation rate when applied in the open state. *C*, currents activated by 30 μM glycine in the WT GlyR are completely inhibited by 100 μM PTX (*left panel*), whereas those activated by 5 μM glycine in the T6′F GlyR are little affected by 300 μM PTX (*center panel*). PTX dose responses in the WT and T6′F GlyRs have been quantitated as described in Ref. 18. The *right panel* shows complete lack of inhibition by 300 μM BB in the T6′F GlyR. This trace is representative of those recorded from 4 cells under the same conditions.

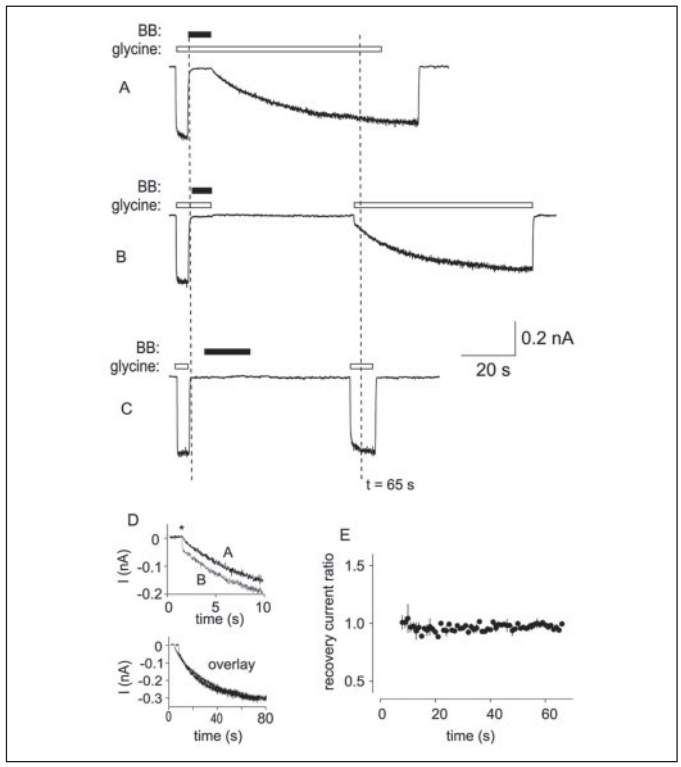

FIGURE 7. **BB trap in the R271C GlyR.** All data in *A–D* were all from the same cell and the experiments in *A–C* were performed exactly as described in the legend to Fig. 4, *B–D*. Glycine was applied throughout at 3 mM and BB at 100 μM. *D*, superimposed initial current recovery phases from *A* and *B*. Traces are aligned according to the time (*asterisk*) that recovery was initiated. *E*, as for *D*, except traces were moved laterally relative to each other until maximum overlap was achieved. Current magnitudes at 1-s intervals were then ratioed, and the results pooled from 3 cells are averaged in *panel E*.

BB. If BB accesses its site equally well in the closed state, the rate at which glycine activates the channels after a closed state BB application should be slowed to a similar extent. To facilitate comparison of glycine-activation rates, the activation segments under each experimental condition (as indicated by numbers *1*, *2*, and *3*) were normalized, superimposed, and expanded in Fig. 6*B*, *upper right panel*. Single exponentials were fit to these curves, and the time constants averaged from 4 cells are averaged in Fig. 6*B*, *lower right panel*. This result demonstrates that BB accesses its binding site in the open state but not the closed state. In contrast, the same experiment performed using PTX demonstrated rapid access to its site in the closed state (12). Thus, BB is a use-dependent inhibitor of recombinant α homomeric GlyRs.

We next sought to determine whether the effects of PTX and BB were mediated by common molecular determinants. The T6′F mutation has previously been shown to drastically reduce the PTX inhibitory potency (18, 29). Sample responses of WT and T6′F mutant GlyR currents to high concentrations of PTX and BB are shown in Fig. 6*C*. We found in each of 4 cells that 300 μM BB had no significant inhibitory effect on currents activated by an EC_{50} concentration (5 μM) of glycine in the T6′F mutant GlyR. Full BB dose responses were not measured in the T6′F GlyR because of its low sensitivity and the limited quantity of the compound. Nevertheless, these results demonstrate a marked similarity in the mechanisms of action of PTX and BB.

The final test was to determine whether BB is trapped in the closed state of the R271C GlyR. The results of this experiment are summarized in Fig. 7. As with PTX inhibition, recovery from BB inhibition was slow (Fig. 7*A*), and the 60-s delay in the addition of glycine indeed demonstrated that BB is trapped in the pore (Fig. 7*B*). Note, however, that the delayed addition of glycine was associated with a small step jump in current that is not present in the corresponding trace in Fig. 7*A*. This effect was observed in all 3 cells in which it was investigated and indicates that BB can escape slowly from its site in the closed state. However, as shown in Fig. 7*C*, BB cannot efficiently reach its inhibitory site in the closed state. To average recovery currents from multiple cells, we first superimposed the recovery currents recorded with and without trap. This is shown in Fig. 7*D*, *upper panel*, where currents are aligned according to the time that glycine-induced recovery was initiated (*asterisk*). This clearly displays the step and the subsequent offset it induces in the recovery phase. To compensate for this offset, the curves were moved laterally to each other until they overlapped maximally (Fig. 7*D*, *lower panel*). The ratio of these currents at 1-s intervals during recovery was then calculated, with the average from 3 cells displayed in Fig. 7*E*. This indicates that apart from the small step current because of slow BB escape, a period of trap does not affect the recovery rate from BB-mediated inhibition.

DISCUSSION

A Binding Site for PTX in the Pore?—PTX significantly slowed the MTSET reaction rate with the A272C, S273C, and L274C GlyRs. Before interpreting this as a PTX-induced conformational change, we must first eliminate the possibility that the effect was because of steric competition between PTX and MTSET. Hence, this discussion first considers the location of the PTX binding site.

PTX has long been thought to bind in the GlyR pore (24, 30). The main evidence in favor of this is that mutations at the 6′ pore-lining position can either abolish PTX sensitivity in the PTX-sensitive α1 GlyR, or drastically enhance PTX sensitivity in the PTX-insensitive $\alpha1\beta$ GlyR (18). The main evidence against a pore binding site hypothesis is that PTX inhibition of the GlyR is not use-dependent. That is, PTX accesses its inhibitory site efficiently in the closed state. Indeed, its inhibitory potency is stronger at low, weakly activating glycine concentrations than at saturating glycine concentrations (12). These characteristics are the opposite of those usually associated with molecules that bind deep in a pore. On the other hand, however, PTX inhibition is use-dependent in the structurally related $GABA_AR$ and GluClRs (10, 11, 17, 22). Furthermore, mutagenesis of a divergent $Ser^{15'}$ residue in the α1 GlyR pore-lining domain back toward the corresponding residues in the $GABA_AR$ β subunit or GluClR β subunit (via the S15′N and S15′Q mutations, respectively) converts PTX into a use-dependent inhibitor of the GlyR (22). Although broadly consistent with a pore binding site for PTX, the above evidence does not constitute a conclusive case for PTX binding in the pore.

We demonstrate here that the R271C GlyR must be opened for PTX to access or leave its binding site. The dissociation rate of PTX is linearly proportional to the open probability over the range 20–100% of its maximum value, but is substantially reduced at lower open probabilities (Fig. 5*C*). These properties are expected if PTX binds in the pore. Similar blocker trap behavior has been observed in a variety of cation-selective channels (31–34), although such phenomena have rarely been described in proteins that do not possess a pore or deep crevice. The present study also shows that mutation of the $Thr^{6'}$ pore-lining residue abolishes sensitivity to both PTX and the structurally unrelated pore blocker, BB. The fact that a single molecular determinant is crucial for the efficacy of both compounds implies that they share a common mode or site of action. Indeed, $Thr^{6'}$ has already been proposed as a PTX contact site, and a molecular modeling study indicates that PTX can plausibly bind in this location (30). Furthermore, by showing that BB is trapped by the R271C GlyR, we demonstrate that the trap effect does not discriminate on the basis of molecular structure. This is consistent with both molecules binding in the pore, but would be difficult to reconcile with them binding to separate sites in an extramembranous part of the protein. Finally, we have previously shown that T6′C is functionally modified by MTSET in the open state only (18). This provides independent evidence for a narrow pore constriction external to T6′C in the closed state. Together, these lines of evidence constitute a strong, but not definitive, case for PTX binding in the pore of the R271C GlyR.

Our experiments do not directly address why BB inhibition of the WT GlyR is use-dependent, whereas PTX inhibition is not. We propose that PTX efficiently accesses its site in the closed state (12) and allosterically inhibits the GlyR by stabilizing a "closed pore" conformation. BB may also have efficient access to the 6′ depth in the closed state, although we propose it requires the channel to be opened for it to bind.

Why is PTX trapped in the pore of the R271C GlyR but not the WT GlyR? The recent structural model of the *Torpedo marmorata* nicotinic acetylcholine receptor transmembrane domains shows a band of hydrophobic residues around the middle of the M2 domain extending from $Leu^{9'}$ to $Val^{13'}$ (8, 35). These residues are linked to the adjacent residues on neighboring subunits by hydrophobic bonds, and thus form a central pore constriction that holds the channel closed. Note that this constriction is not necessarily the gate that controls ion flow. Evidence from substituted cysteine accessibility studies implies that the ion gate lies in the −2′ to 2′ region in the nicotinic acetylcholine receptor and $GABA_AR$ (36–38), although it may be centrally located in the 5-hydroxytryptamine type 3-gated cation channel (39, 40). We propose that the centrally located gate does not form a substantial barrier to PTX access in the WT GlyR in the closed state. However, PTX is converted into a use-dependent inhibitor of the GlyR by mutations to $Ser^{15'}$ (22) and to R271C and K276C in the M2–M3 loop (present study). We propose that these mutations disrupt M2 structure, leading to an even smaller constriction at the pore midpoint. Thus, the pore must be opened to permit the passage of large molecules like PTX. The idea that changes in conformation of the M2–M3 loop lead to a conformational change at the pore midpoint is a common feature of all models proposed so far to explain LGIC activation (3, 41–44).

A PTX-specific Conformation Change—By binding in the pore, PTX cannot sterically hinder MTSET from reacting with M2–M3 loop cysteines. We therefore conclude that PTX changes the MTSET reaction rate by changing the intrinsic reactivity rates of the introduced cysteines. This study has shown that a given relative peak current magnitude (or EC value) is associated with a fixed cysteine reaction rate for each mutant GlyR. Because PTX changes the relationship between EC and cysteine reactivity, we conclude that it alters the M2–M3 loop structure in a way that cannot be achieved by glycine.

This conclusion has important implications for our understanding of LGIC activation mechanisms. Our current understanding is that agonist binding causes a conformational change in the extracellular ligand-binding domain and this is transmitted to the channel gate via conformational changes in the M2–M3 loop (2, 3, 43, 44). Because allosterically acting modulators also cause global changes in receptor conformation, it is expected that these should also alter M2–M3 loop conformation. However, until now there has been no evidence to suggest that allosteric modulators could act in any other way than by stabilizing the M2–M3 loop in either the glycine-liganded open conformation or the glycine-free closed conformation.

Thus, the crucial insight of this study is that PTX can alter the conformation of the GlyR M2–M3 loop in a way that cannot be achieved by simply varying the glycine concentration alone. This result reveals a hitherto unexpected complexity in the role of the M2–M3 loop. Our results also validate the R271C GlyR as a tool for establishing whether or not molecules bind in the pore.

REFERENCES

1. Legendre, P. (2001) *Cell. Mol. Life Sci.* **58,** 760–793
2. Lynch, J. W. (2004) *Physiol. Rev.* **84,** 1051–1095
3. Unwin, N. (2003) *FEBS Lett.* **555,** 91–95
4. Barry, P. H., and Lynch, J. W. (2005) *IEEE Trans. Nanobiosci.* **4,** 70–80
5. Lynch, J. W., Rajendra, S., Pierce, K. D., Handford, C. A., Barry, P. H., and Schofield, P. R. (1997) *EMBO J.* **16,** 110–120
6. Grosman, C., Zhou, M., and Auerbach, A. (2000) *Nature* **403,** 773–776
7. Kash, T. L., Jenkins, A., Kelley, J. C., Trudell, J. R., and Harrison, N. L. (2003) *Nature* **421,** 272–275
8. Miyazawa, A., Fujiyoshi, Y., and Unwin, N. (2003) *Nature* **424,** 949–955
9. Lynch, J. W., Han, N. L., Haddrill, J., Pierce, K. D., and Schofield, P. R. (2001) *J. Neurosci.* **21,** 2589–2599
10. Newland, C. F., and Cull-Candy, S.G. (1992) *J. Physiol.* **447,** 191–213
11. Etter, A., Cully, D. F., Liu, K. K., Reiss, B., Vassilatis, D. K., Schaeffer, J. M., and Arena, J. P. (1999) *J. Neurochem.* **72,** 318–326
12. Lynch, J. W., Rajendra, S., Barry, P. H., and Schofield, P. R. (1995) *J. Biol. Chem.* **270,** 13799–13806
13. Ffrench-Constant, R. H., Rocheleau, T. A., Steichen, J. C., and Chalmers, A. E. (1993)

Nature **363,** 449–451
14. Gurley, D., Amin, J., Ross, P. C., Weiss, D. S., and White, G. (1995) *Receptors Channels* **3,** 13–20
15. Wang, T. L., Hackam, A. S., Guggino, W. B., and Cutting, G. R. (1995) *Proc. Natl. Acad. Sci. U. S. A.* **92,** 11751–11755
16. Zhang, D., Pan, Z. H., Zhang, X., Brideau, A. D., and Lipton, S. A. (1995) *Proc. Natl. Acad. Sci. U. S. A.* **92,** 11756–11760
17. Xu, M., Covey, D. F., and Akabas, M. H. (1995) *Biophys. J.* **69,** 1858–1867
18. Shan, Q., Haddrill, J. L., and Lynch, J. W. (2001) *J. Neurochem.* **76,** 1109–1120
19. Legendre, P. (1997) *J. Neurophysiol.* **77,** 2400–2415
20. Qian, H., Pan, Y., Zhu, Y., and Khalili, P. (2005) *Mol. Pharmacol.* **67,** 470–479
21. Yoon, K. W., Covey, D. F., and Rothman, S. M. (1993) *J. Physiol.* **464,** 423–439
22. Dibas, M. I., Gonzales, E. B., Das, P., Bell-Horner, C. L., and Dillon, G. H. (2002) *J. Biol. Chem.* **277,** 9112–9117
23. Chang, Y., and Weiss, D. S. (2002) *Nat. Neurosci.* **5,** 1163–1168
24. Pribilla, I., Takagi, T., Langosch, D., Bormann, J., and Betz, H. (1992) *EMBO J.* **11,** 4305–4311
25. Beato, M., Groot-Kormelink, P. J., Colquhoun, D., and Sivilotti, L. G. (2002) *J. Gen. Physiol.* **119,** 443–466
26. Rundstrom, N., Schmieden, V., Betz, H., Bormann, J., and Langosch, D. (1994) *Proc. Natl. Acad. Sci. U. S. A.* **91,** 8950–8954
27. Kondratskaya, E. L., Lishko, P. V., Chatterjee, S. S., and Krishtal, O. A. (2002) *Neurochem. Int.* **40,** 647–653
28. Ivic, L., Sands, T. T., Fishkin, N., Nakanishi, K., Kriegstein, A. R., and Stromgaard, K. (2003) *J. Biol. Chem.* **278,** 49279–49285
29. Shan, Q., Haddrill, J. L., and Lynch, J. W. (2002) *J. Biol. Chem.* **277,** 44845–44853
30. Zhorov, B. S., and Bregestovski, P. D. (2000) *Biophys. J.* **78,** 1786–1803
31. Armstrong, C. M. (1971) *J. Gen. Physiol.* **58,** 413–437
32. Miller, C. (1987) *Biophys. J.* **52,** 123–126
33. Holmgren, M., Smith, P. L., and Yellen, G. (1997) *J. Gen. Physiol.* **109,** 527–535
34. Phillips, L. R., and Nichols, C. G. (2003) *J. Gen. Physiol.* **122,** 795–804
35. Unwin, N. (2005) *J. Mol. Biol.* **346,** 967–989
36. Xu, M., and Akabas, M. H. (1996) *J. Gen. Physiol.* **107,** 195–205
37. Akabas, M. H., Kaufmann, C., Archdeacon, P., and Karlin, A. (1994) *Neuron* **13,** 919–927
38. Wilson, G. G., and Karlin, A. (1998) *Neuron* **20,** 1269–1281
39. Panicker, S., Cruz, H., Arrabit, C., and Slesinger, P. A. (2002) *J. Neurosci.* **22,** 1629–1639
40. Panicker, S., Cruz, H., Arrabit, C., Suen, K. F., and Slesinger, P. A. (2004) *J. Biol. Chem.* **279,** 28149–28158
41. Horenstein, J., Wagner, D. A., Czajkowski, C., and Akabas, M. H. (2001) *Nat. Neurosci.* **4,** 477–485
42. Karlin, A. (2002) *Nat. Rev. Neurosci.* **3,** 102–114
43. Auerbach, A. (2003) *Sci. STKE* 2003, RE11
44. Kash, T. L., Trudell, J. R., and Harrison, N. L. (2004) *Biochem. Soc. Trans.* **32,** 540–546

A Picrotoxin-specific Conformational Change in the Glycine Receptor M2–M3 Loop

Rebecca Hawthorne and Joseph W. Lynch

J. Biol. Chem. 2005, 280:35836-35843.
doi: 10.1074/jbc.M506645200 originally published online August 18, 2005
